

Pion observables in Minkowski space.

Wayne de Paula

Instituto Tecnológico de Aeronáutica - Brasil

Collaborators

D. Duarte, E. Ydrefors, T. Frederico, G. Salmè and O. Oliveira

Oficina Nacional de Teoria Quântica de Campos - 2021

wayne@ita.br

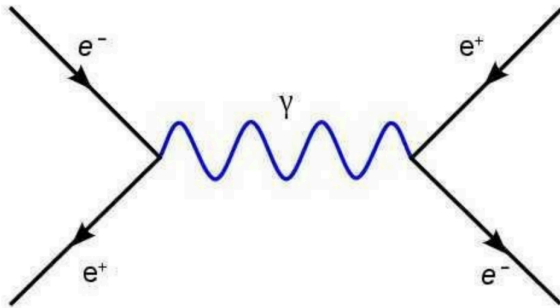


Outline

- I. Some properties of QCD
- II. Nonperturbative methods for QCD
- III. Pion as a fermion anti-fermion bound state in Minkowski space.
- IV. Nakanishi integral representation and LF projection.
- V. Valence Momentum Distributions, Valence Probability.
- VI. Decay constant, charge radius and Electromagnetic Form Factor.
- VII. Conclusions and perspectives

QED vs QCD

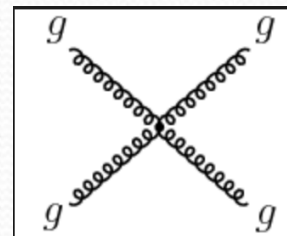
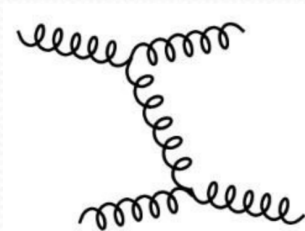
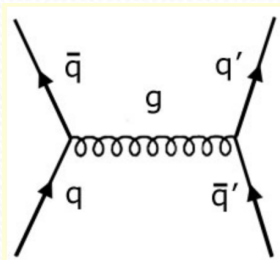
Photons are neutral



There are no photon self-interaction

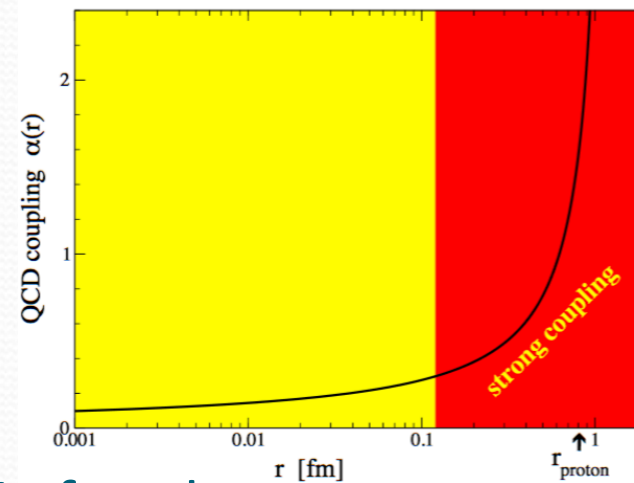
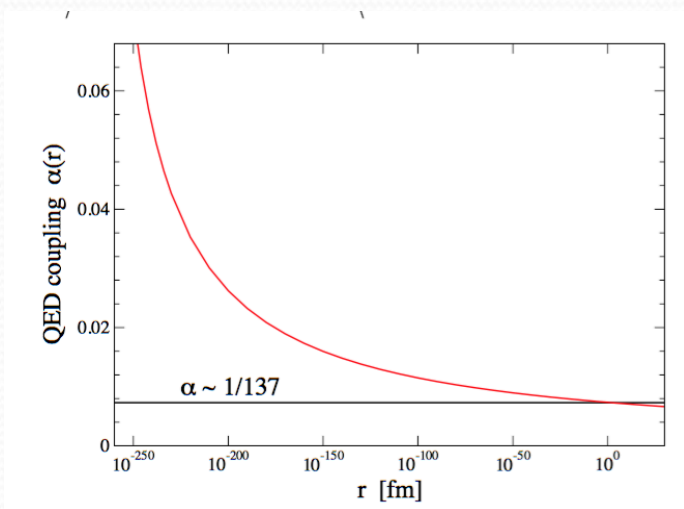
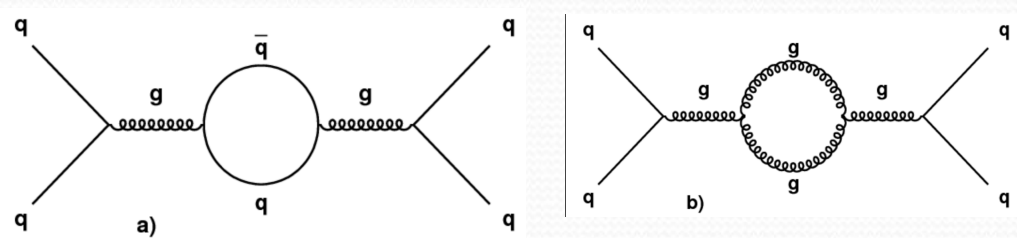
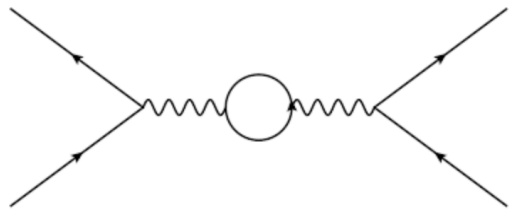
Gluons have color charge

There are gluon self-interaction



QED vs QCD

Quantum fluctuations: coupling depends on the scale.



Asymptotic freedom
Nobel Prize 2004
Gross, Politzer & Wilczek

1fm= 10^{-15} m

Nonperturbative QCD

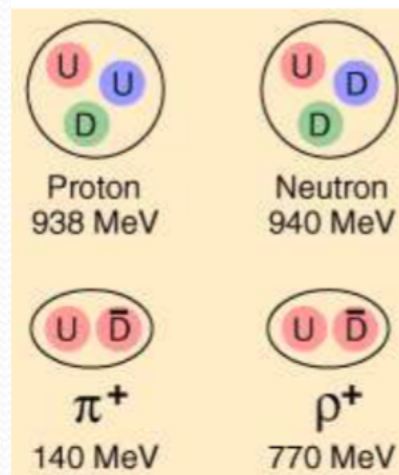
For a quantitative understanding of hadron physics, we need nonperturbative methods to study QCD at low energies.

- Hadron mass spectrum

Pion mass ~ 140 MeV

Rho mass ~ 770 MeV

Nucleon mass ~ 1 GeV



Perturbative QCD: quarks u and d ~ 5 MeV

- Structure of Hadrons: Hadron Tomography
- Confinement: Experimentally, only color-singlet hadrons are observed
No free quarks have been observed

Conjecture: Colored objects are confined inside the hadrons

Nonperturbative approaches to QCD

- Lattice QCD

Generating functional $Z[J] = \int \mathcal{D}A \mathcal{D}\psi \mathcal{D}\bar{\psi} e^{iS}$

Simulate QCD action

Discretize (Euclidean) space-time

Wick-rotation: $t \rightarrow it$ $Z[J] = \int \mathcal{D}A \mathcal{D}\psi \mathcal{D}\bar{\psi} e^{-S}$

Use Monte Carlo methods to sample path integrals

Equivalent to a Statistical Mechanics problem

Finite lattice size and spacing effects

Need extrapolation methods for the continuum limit $L \rightarrow \infty, a \rightarrow 0$

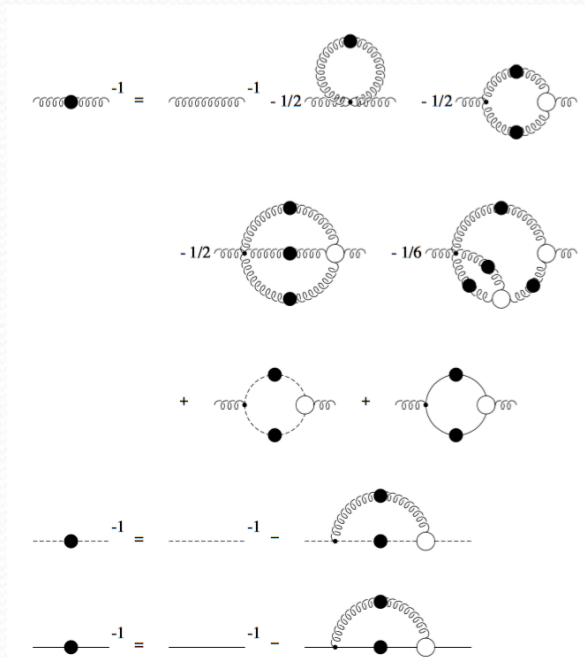
Requires massive computational power.

Nonperturbative approaches to QCD

- Schwinger-Dyson Equations

Generating functional $Z[J] = \int \mathcal{D}A \mathcal{D}\psi \mathcal{D}\bar{\psi} e^{iS}$

Field equations can be derived from the generating functional



EoM form infinite hierarchy of coupled integral equations for the Green functions

Reduce to pQCD in weak coupling limit

Truncation is needed

- QCD in Coulomb Gauge

Meson 2^- and B_c spectrum.

Challenge: Minkowski Calculations

Most non-perturbative methods are formulated in Euclidean space

It is not easy to connect the Euclidean calculations with Structure functions defined in Minkowski Space.

Wick Rotation: We have to be care with the presence of singularities.

Minkowski solutions: Bethe-Salpeter
Schwinger-Dyson

Schwinger-Dyson equation in Rainbow ladder truncation

Minkowski space

In collaboration with Duarte, Frederico, Ydrefors

QED-like, bare vertices, massive vector boson, Pauli-Villars regulator

The rainbow ladder Schwinger-Dyson equation in **Minkowski** space is

$$S_f^{-1}(k) = \not{k} - \bar{m}_0 + ig^2 \int \frac{d^4q}{(2\pi)^4} \gamma_\mu S_f(k-q) \gamma_\nu D^{\mu\nu}(q)$$

The massive gauge boson is given by

$$D^{\mu\nu}(q) = \frac{1}{q^2 - m_\sigma^2 + i\epsilon} \left[g^{\mu\nu} - \frac{(1-\xi)q^\mu q^\nu}{q^2 - \xi m_\sigma^2 + i\epsilon} \right]$$

$\xi = 0$ (Landau Gauge) & $\xi = 1$ (Feynman Gauge)

The dressed fermion propagator is

$$S_f(k) = \frac{1}{k - m_B + kA_f(k^2) - B_f(k^2) + i\epsilon}$$

Also discussed in V. Sauli, JHEP 0302, 001 (2003)

Fermion Schwinger-Dyson equation (Rainbow ladder)

Self-Energies Integral representations

$$A_f(k^2) = \int_0^\infty d\gamma \frac{\rho_A(\gamma)}{k^2 - \gamma + i\epsilon} \quad B_f(k^2) = \int_0^\infty d\gamma \frac{\rho_B(\gamma)}{k^2 - \gamma + i\epsilon}$$

Vector and scalar Self-Energy densities

Fermion propagator – Integral representation

$$S_f = R \frac{\not{k} + \bar{m}_0}{k^2 - \bar{m}_0^2 + i\epsilon} + \not{k} \int_0^\infty d\gamma \frac{\rho_v(\gamma)}{k^2 - \gamma + i\epsilon} + \int_0^\infty d\gamma \frac{\rho_s(\gamma)}{k^2 - \gamma + i\epsilon}$$

physical mass

Vector and scalar spectral densities

$$\begin{aligned} \not{k}A(k^2) - B(k^2) &= ig^2 \int \frac{d^4q}{(2\pi)^4} \frac{\gamma_\mu S(k-q)\gamma_\nu}{q^2 - m_\sigma^2 + i\epsilon} \left[g^{\mu\nu} - \frac{(1-\xi)q^\mu q^\nu}{q^2 - \xi m_\sigma^2 + i\epsilon} \right] \\ &\quad - ig^2 \int \frac{d^4q}{(2\pi)^4} \frac{\gamma_\mu S(k-q)\gamma_\nu}{q^2 - \Lambda^2 + i\epsilon} \left[g^{\mu\nu} - \frac{(1-\xi)q^\mu q^\nu}{q^2 - \xi \Lambda^2 + i\epsilon} \right] \end{aligned}$$

Gauge fixing

Pauli-Villars regulator

Fermion Schwinger-Dyson equation (Rainbow ladder)

- Parameters: $\alpha = \frac{g^2}{4\pi}$, Λ , m_σ , \bar{m}_0 .
- Self energy densities: $\rho_A(\gamma) = -\text{Im}[A(\gamma)]/\pi$ and $\rho_B(\gamma) = -\text{Im}[B(\gamma)]/\pi$.
- Solutions of DSE obtained writing the trivial relation $S_f^{-1}S_f = 1$ in a suitable form:

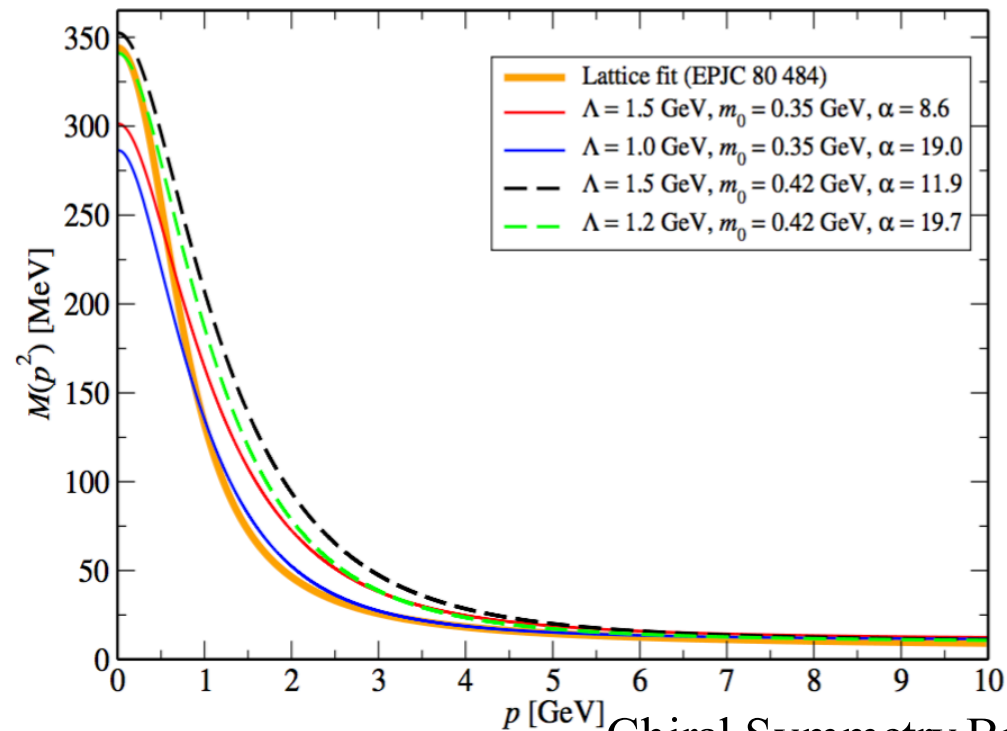
$$\frac{R}{k^2 - \bar{m}_0^2 + i\epsilon} + \int_0^\infty d\gamma \frac{\rho_v(\gamma)}{k^2 - \gamma + i\epsilon} = \frac{1 + A_f(k^2)}{k^2(1 + A_f(k^2))^2 - (m_B + B_f(k^2))^2 + i\epsilon}$$
$$\frac{R\bar{m}_0}{k^2 - \bar{m}_0^2 + i\epsilon} + \int_0^\infty d\gamma \frac{\rho_s(\gamma)}{k^2 - \gamma + i\epsilon} = \frac{m_B + B_f(k^2)}{k^2(1 + A_f(k^2))^2 - (m_B + B_f(k^2))^2 + i\epsilon}$$

Phenomenological Model (Recent Developments)

In collaboration with Duarte, Frederico, Ydrefors

We can calibrate the model to reproduce Lattice Data for $M(p^2)$

$$M^2(p^2) = \frac{B^2(p^2)}{A^2(p^2)}$$
$$Z(p^2) = \frac{1}{A(p^2)}$$



Chiral Symmetry Breaking

The next step is to use this solution to obtain the Fermion Anti-Fermion bound state

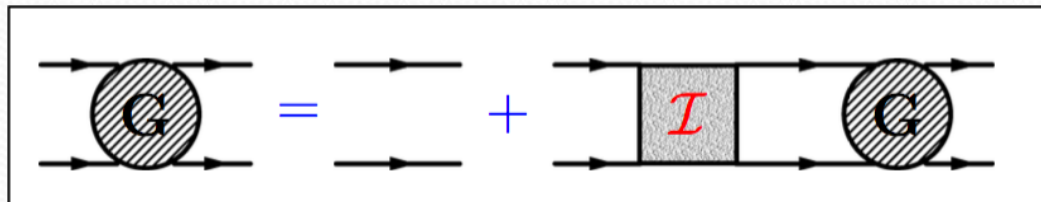
Bound State

We start from the four-point Green function

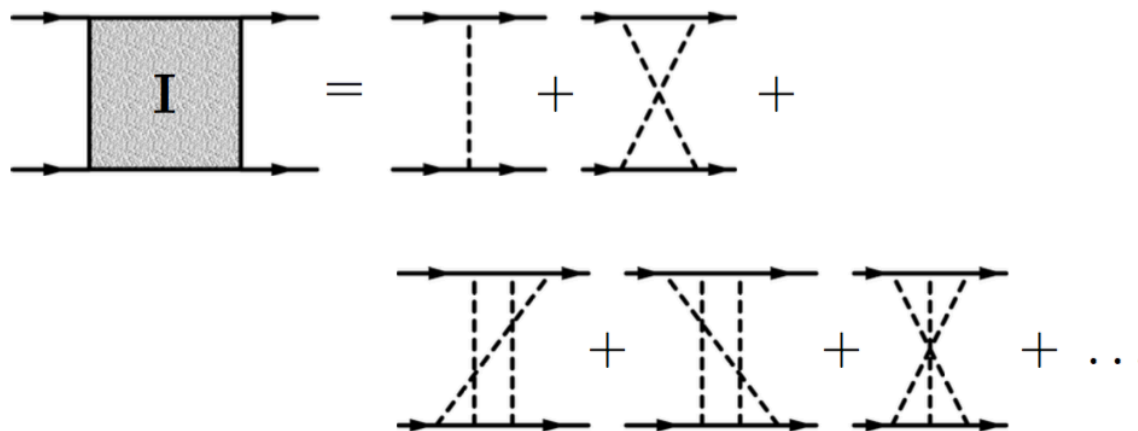
$$G(x_1, x_2; y_1, y_2) = \langle 0 | T \{ \phi_1(x_1) \phi_2(x_2) \phi_1^+(y_1) \phi_2^+(y_2) \} | 0 \rangle$$

which is a solution of the integral equation

$$G = G_0 + G_0 \mathcal{I} G$$



$\mathcal{I} \equiv$ kernel given by the infinite sum of irreducible Feynmann graphs



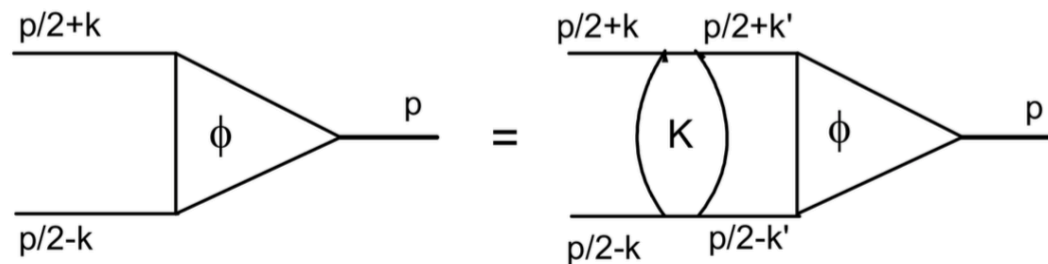
Iterations produce all the expected contributions

Bethe-Salpeter Equation

Close to the bound-state pole we obtain the BSE

$$\phi(k; p_B) = G_0(k; p_B) \int d^4k' \mathcal{I}(k, k'; p_B) \phi(k'; p_B)$$

BSA in configuration space: $\phi(x_1, x_2; p_B) = \langle 0 | T \{ \phi_1(x_1) \phi_2(x_2) \} | p_B \rangle$

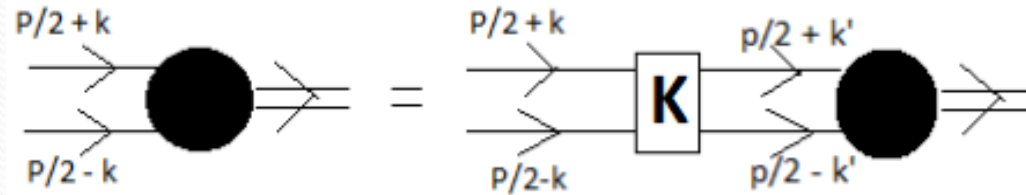


The same Kernel of the four-point Green function

Challenge: To solve the BSE in Minkowski space

Quark-antiquark bound state - Pion

- Bethe-Salpeter equation (0^-) :



$$\Phi(k; P) = S(k + \frac{P}{2}) \int \frac{d^4 k'}{(2\pi)^4} S^{\mu\nu}(q) \Gamma_\mu(q) \Phi(k'; P) \hat{\Gamma}_\nu(q) S(k - \frac{P}{2})$$

$$\hat{\Gamma}_\nu(q) = C \Gamma_\nu(q) C^{-1}$$

where we use: i) bare propagators for the quarks and gluons;
ii) ladder approximation

$$S(P) = \frac{i}{\not{P} - m + i\epsilon} \quad S^{\mu\nu}(q) = -i \frac{g^{\mu\nu}}{q^2 - \mu^2 + i\epsilon}$$

$$\text{Quark-gluon vertex} \quad \Gamma^\mu = ig \frac{\mu^2 - \Lambda^2}{q^2 - \Lambda^2 + i\epsilon} \gamma^\mu$$

We consider only one of the Longitudinal components of the QGV

We set the value of the scale parameter (~ 300 MeV) from the combined analysis of Lattice simulations, the Quark-Gap Equation and Slanov-Taylor identity.

Nakanishi Integral Representation

- Nakanishi representation: Generalization of the Källén-Lehman integral representation (two point functions) for n-point functions. The denominator carries the overall analytical behavior in Minkowski space.

Bethe-Salpeter amplitude

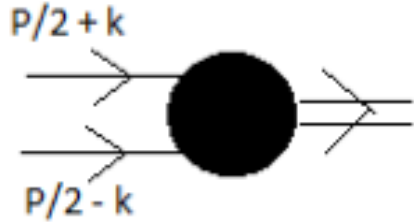
$$\Phi(k, p) = \int_{-1}^1 dz' \int_0^\infty d\gamma' \frac{g(\gamma', z')}{(\gamma' + \kappa^2 - k^2 - p \cdot kz' - i\epsilon)^3}$$

BSE in Minkowski space with NIR

- Kusaka and Williams, PRD 51 7026 (1995); Karmanov and Carbonell, EPJA 27 1 (2006), EPJA 27 11 (2006), EPJA 27 11 (2010);
- Frederico, Salme and Viviani PRD 85 036009 (2012), PRD 89, 016010 (2014).
- WP, Frederico, Salme and Viviani PRD 94 071901 (2016).
- WP, Frederico, Salme, Viviani and Pimentel EPJC 77 764 (2017).
- WP, Ydrefors, A. Nogueira, Frederico and Salme PRD 103 014002 (2021).
- Ydrefors, WP, Nogueira, Frederico and Salme PLB 820, 136494 (2021).

NIR for fermion-antifermion Bound State

BSA for a quark-antiquark bound state



$$\Phi(k, p) = \sum_{i=1}^4 S_i(k, p) \phi_i(k, p)$$

$$S_1 = \gamma_5 \quad S_2 = \frac{1}{M} \not{p} \gamma_5 \quad S_3 = \frac{k \cdot p}{M^3} \not{p} \gamma_5 - \frac{1}{M} \not{k} \gamma_5 \quad S_4 = \frac{i}{M^2} \sigma_{\mu\nu} p^\mu k^\nu \gamma_5$$

Using the NIR for the scalar functions

$$\phi_i(k, p) = \int_{-1}^{+1} dz' \int_0^\infty d\gamma' \frac{g_i(\gamma', z')}{(k^2 + p \cdot k z' + M^2/4 - m^2 - \gamma' + i\epsilon)^3}$$

System of coupled integral equations

$$\int_{-1}^1 dz' \int_0^\infty d\gamma' \frac{g_i(\gamma', z')}{[k^2 + z' p \cdot k - \gamma' - \kappa^2 + i\epsilon]^3} = \sum_j \int_{-1}^1 dz' \int_0^\infty d\gamma' \mathcal{K}_{ij}(k, p; \gamma', z') g_j(\gamma', z')$$

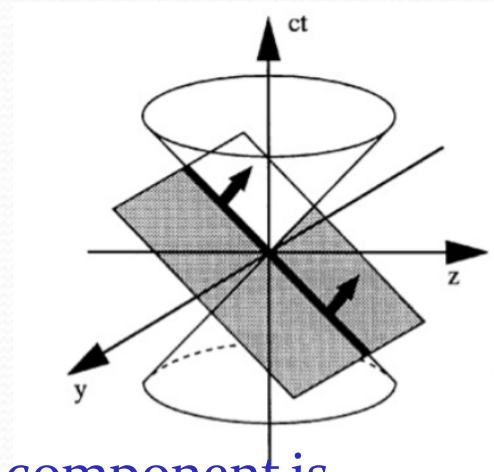
Projecting BSE onto the LF hyper-plane $x^+=0$

Light-Front variables $x^\mu = (x^+, x^-, \mathbf{x}_\perp)$

$$\text{LF-time } x^+ = x^0 + x^3$$

$$x^- = x^0 - x^3$$

$$\mathbf{x}_\perp = (x^1, x^2)$$



Within the LF framework, the valence component is obtained by integrating the BSA on k .

$$\text{LF amplitudes } \left| \psi_i(\gamma, \xi) = \int \frac{dk^-}{2\pi} \phi_i(k, p) = -\frac{i}{M} \int_0^\infty d\gamma' \frac{g_i(\gamma', z)}{[\gamma + \gamma' + m^2 z^2 + (1 - z^2)\kappa^2]^2} \right.$$

The coupled equation system is

$$\int_0^\infty d\gamma' \frac{g_i(\gamma', z')}{[\gamma + \gamma' + m^2 z^2 + (1 - z^2)\kappa^2]^2} = iMg^2 \sum_j \int_0^\infty d\gamma' \int_{-1}^1 dz' \mathcal{L}_{ij}(\gamma, z; \gamma' z') g_j(\gamma, z')$$

The Kernel contains singular contributions

NIR for two-fermions

WP, Frederico, Salmè, Viviani, **PRD94** (2016) 071901

We can single out the singular contributions

For two-fermion BSE

$$C_j = \int_{-\infty}^{\infty} \frac{dk^-}{2\pi} (k^-)^j \mathcal{S}(k^-, v, z, z', \gamma, \gamma')$$

with $j=1,2,3$ and in the worst case

$$\mathcal{S}(k^-, v, z, z', \gamma, \gamma') \sim \frac{1}{[k^-]^2} \quad \text{for } k^- \rightarrow \infty$$

Then one can not close the arc at the infinity .

The severity of the singularities (power j), does not depend on the Kernel

We calculate the singular contribution using

$$\int_{-\infty}^{\infty} dx \frac{1}{[\beta x - y \mp i\epsilon]^2} = \pm (2\pi)i \frac{\delta(\beta)}{[-y \mp i\epsilon]} \quad \text{Yan PRD 7 (1973) 1780}$$

Numerical Method

Basis expansion for the Nakanishi weight function

$$g_i(\gamma, z) = \sum_{m=0}^{\infty} \sum_{n=0}^{\infty} w_{mn}^i G_{2m+r_i}^{\lambda_i}(z) \mathcal{J}_n(\gamma)$$

Gegenbauer polynomials

$$G_n^\lambda(z) = (1 - z^2)^q \Gamma(\lambda) \sqrt{\frac{n!(n + \lambda)}{2^{1-2\lambda} \pi \Gamma(n + 2\lambda)}} C_n^\lambda(z)$$

Laguerre polynomials

$$\mathcal{J}_n(\gamma) = \sqrt{a} L_n(a\gamma) e^{-a\gamma/2}$$

We obtain a discrete generalized eigenvalue problem

$$C \mathbf{w} = g^2 D \mathbf{w}$$

We used ~ 44 Laguerre polynomials and 44 Gegenbauer

Normalization

In order to calculate hadronic properties, we need to properly normalize the BSA

$$\text{Tr} \left[\int \frac{d^4k}{(2\pi)^4} \bar{\Phi}(k, p) \frac{\partial}{\partial p'^\mu} \{S^{-1}(k + p'/2) \Phi(k, p) S^{-1}(k - p'/2)\} \Big|_{p'=p; p^2=M^2} \right] = -i 2p_\mu$$

Using the BSA expansion and performing the Dirac traces, we have

$$i \int \frac{d^4k}{(2\pi)^4} \left[\phi_1\phi_1 + \phi_2\phi_2 + b\phi_3\phi_3 + b\phi_4\phi_4 - 4 b\phi_1\phi_4 - 4 \frac{m}{M} \phi_2\phi_1 \right] = 1$$

From the NIR, we obtain

$$\begin{aligned} & \frac{3}{32\pi^2} \int_{-1}^{+1} dz' \int_0^\infty d\gamma' \int_{-1}^{+1} dz \int_0^\infty d\gamma \int_0^1 dv \frac{v^2(1-v)^2}{[\kappa^2 + \frac{M^2}{4}\lambda^2 + \gamma'v + \gamma(1-v) - i\eta]^4} \\ & \times \left\{ g_1(\gamma', z') g_1(\gamma, z) + g_2(\gamma', z') g_2(\gamma, z) - 4 \frac{m}{M} g_2(\gamma', z') g_1(\gamma, z) \right. \\ & \left. + \frac{[\kappa^2 + \frac{M^2}{4}\lambda^2 + \gamma'v + \gamma(1-v) - i\eta]}{2M^2} \right. \\ & \left. \times [g_3(\gamma', z') g_3(\gamma, z) + g_4(\gamma', z') g_4(\gamma, z) - 4g_1(\gamma', z') g_4(\gamma, z)] \right\} = -1 \end{aligned}$$

LF Momentum Distributions

The fermionic field on the null-plane is given by:

$$\psi^{(+)}(\tilde{x}, x^+ = 0^+) = \int \frac{d\tilde{q}}{(2\pi)^{3/2}} \frac{\theta(q^+)}{\sqrt{2q^+}} \sum_{\sigma} \left[U^{(+)}(\tilde{q}, \sigma) b(\tilde{q}, \sigma) e^{i\tilde{q} \cdot \tilde{x}} + V^{(+)}(\tilde{q}, \sigma) d^{\dagger}(\tilde{q}, \sigma) e^{-i\tilde{q} \cdot \tilde{x}} \right]$$

where

$$U^{(+)}(\tilde{q}, \sigma) = \Lambda^+ u(\tilde{q}, \sigma) \quad , \quad V^{(+)}(\tilde{q}, \sigma) = \Lambda^+ v(\tilde{q}, \sigma) \quad \Lambda^{\pm} = \frac{1}{4} \gamma^{\mp} \gamma^{\pm}$$

Hence d^{\dagger} and b are the fermion creation/annihilation operators

The LF valence amplitude is the Fock component with the lowest number of constituents

$$\varphi_2(\xi, \mathbf{k}_{\perp}, \sigma_i; M, J^{\pi}, J_z) = (2\pi)^3 \sqrt{N_c} 2p^+ \sqrt{\xi(1-\xi)} \times \langle 0 | b(\tilde{q}_2, \sigma_2) d(\tilde{q}_1, \sigma_1) | \tilde{p}, M, J^{\pi}, J_z \rangle ,$$

$$\text{where } \tilde{q}_1 \equiv \{q_1^+ = M(1-\xi), -\mathbf{k}_{\perp}\}, \tilde{q}_2 \equiv \{q_2^+ = M\xi, \mathbf{k}_{\perp}\} \text{ and } \xi = 1/2 + k^+/p^+.$$

LF Momentum Distributions

LF valence amplitude in terms of BS amplitude is:

$$\varphi_2(\xi, \mathbf{k}_\perp, \sigma_i; M, J^\pi, J_z) = \frac{\sqrt{N_c}}{p^+} \frac{1}{4} \bar{u}_\alpha(\tilde{q}_2, \sigma_2) \int \frac{dk^-}{2\pi} [\gamma^+ \Phi(k, p) \gamma^+]_{\alpha\beta} v_\beta(\tilde{q}_1, \sigma_1).$$

which can be decomposed into two spin contributions:

Anti-aligned configuration:

$$\psi_{\uparrow\downarrow}(\gamma, z) = \psi_2(\gamma, z) + \frac{z}{2} \psi_3(\gamma, z) + \frac{i}{M^3} \int_0^\infty d\gamma' \frac{\partial g_3(\gamma', z) / \partial z}{\gamma + \gamma' + z^2 m^2 + (1 - z^2) \kappa^2}$$

Aligned configuration: $\psi_{\uparrow\uparrow}(\gamma, z) = \psi_{\downarrow\downarrow}(\gamma, z) = \frac{\sqrt{\gamma}}{M} \psi_4(\gamma, z)$

with the LF amplitudes given by

$$\psi_i(\gamma, z) = -\frac{i}{M} \int_0^\infty d\gamma' \frac{g_i(\gamma', z)}{[\gamma + \gamma' + m^2 z^2 + (1 - z^2) \kappa^2]^2}$$

Valence Probability

We can define the Valence Probability as

$$P_{val} = \frac{1}{(2\pi)^3} \sum_{\sigma_1 \sigma_2} \int_{-1}^1 \frac{dz}{(1-z^2)} \int d\mathbf{k}_\perp$$
$$\times \left| \varphi_{n=2}(\xi, \mathbf{k}_\perp, \sigma_i; M, J^\pi, J_z) \right|^2 \quad \text{where } z = 1 - 2\xi$$

The probability to find the valence component in the bound state

The **Valence momentum** distribution density is

$$P_{val} = \int_{-1}^1 dz \int_0^\infty d\gamma \mathcal{P}_{val}(\gamma, z)$$

We decompose in terms of the aligned and anti-aligned LFWF:

$$\mathcal{P}_{val}(\gamma, z) = \frac{N_c}{16\pi^2} \left[|\psi_{\uparrow\downarrow}(\gamma, z)|^2 + |\psi_{\uparrow\uparrow}(\gamma, z)|^2 \right]$$

Quantitative results: Static properties

WP, Ydrefors, A. Nogueira, Frederico and Salme PRD 103 014002 (2021).

Set	m (MeV)	B/m	μ/m	Λ/m	P_{val}	$P_{\uparrow\downarrow}$	$P_{\uparrow\uparrow}$	f_π (MeV)
I	187	1.25	0.15	2	0.64	0.55	0.09	77
II	255	1.45	1.5	1	0.65	0.55	0.10	112
III	255	1.45	2	1	0.66	0.56	0.11	117
IV	215	1.35	2	1	0.67	0.57	0.11	98
V	187	1.25	2	1	0.67	0.56	0.11	84
VI	255	1.45	2.5	1	0.68	0.56	0.11	122
VII	255	1.45	2.5	1.1	0.69	0.56	0.12	127
VIII	255	1.45	2.5	1.2	0.70	0.57	0.13	130
IX	255	1.45	1	2	0.70	0.57	0.14	134
X	215	1.35	1	2	0.71	0.57	0.14	112
XI	187	1.25	1	2	0.71	0.58	0.14	96

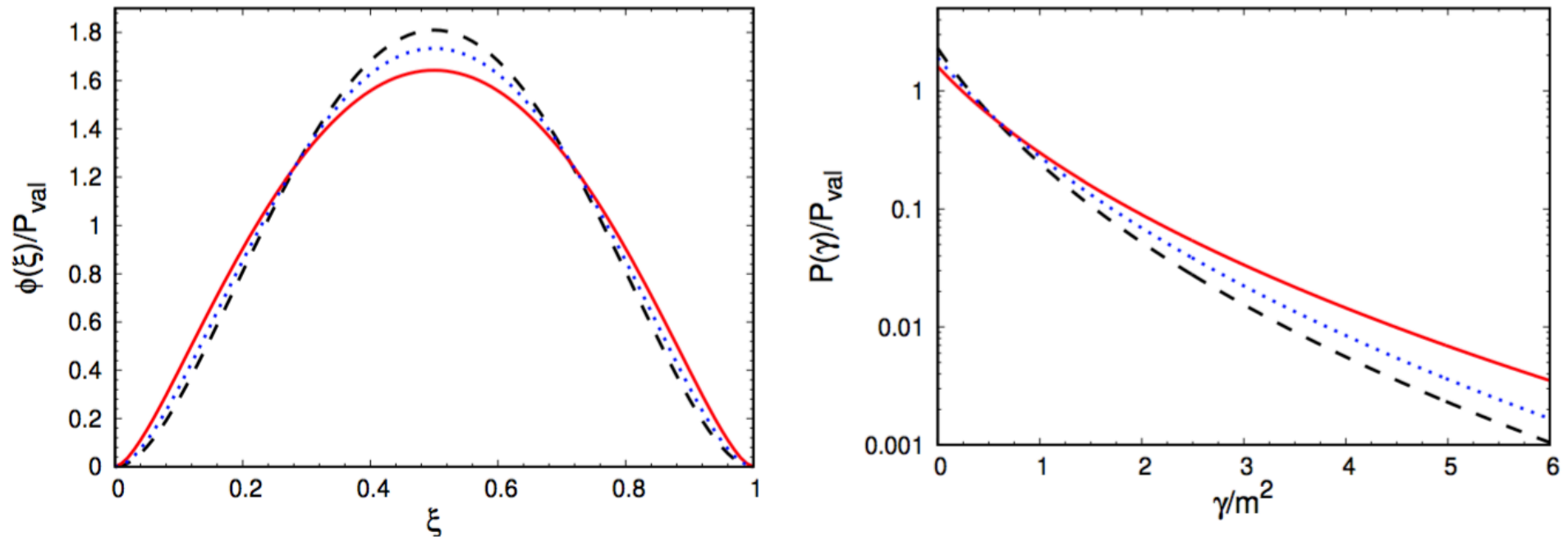
The set VIII reproduces the pion decay constant

$$m_q = 255 \text{ MeV}, m_g = 637.5 \text{ MeV and } \Lambda = 306 \text{ MeV}$$

The contributions beyond the valence component are important, $\sim 30\%$

Valence LF-Momentum Distributions

WP, Ydrefors, A. Nogueira, Frederico and Salme **PRD** 103 014002 (2021).



Result in red reproduce experimental f_π and two other cases shown for comparison.

Here

$$\phi(\xi) = \int_0^\infty d\gamma \mathcal{P}(\gamma, z), \quad P(\gamma) = \int_{-1}^1 dz \mathcal{P}(\gamma, z)$$

where $P(\gamma, z)$ is valence probability distribution.

$\phi(\xi)$ is pdf at initial scale. Evolved PDFs are in progress.

Pion image on the null-plane

The probability distribution of the quarks inside the pion, on the light-front, is evaluated in the space given by the Cartesian product of the Ioffe-time and the plane spanned by the transverse coordinates.

Our goal is to use the configuration space in order to have a more detailed information of the space-time structure of the hadrons.

The Ioffe-time is useful for studying the relative importance of short and long light-like distances. It is defined as:

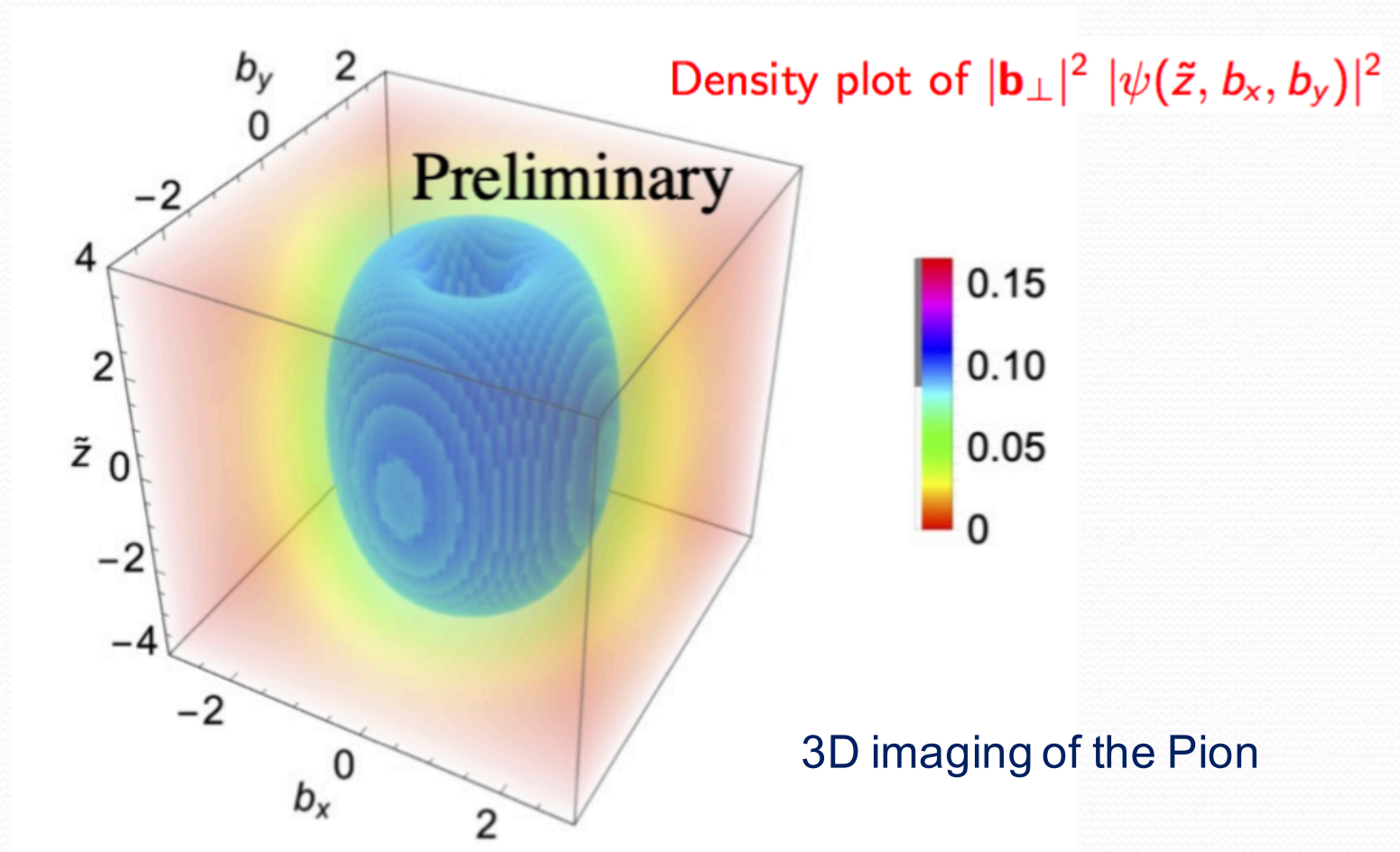
$$\tilde{z} = x \cdot P_{target} = x^- P_{target}^+ / 2 \quad \text{on the hyperplane } x^+ = 0$$

Pion image on the null-plane

WP, Ydrefors, A. Nogueira, Frederico and Salme **PRD** 103 014002 (2021).

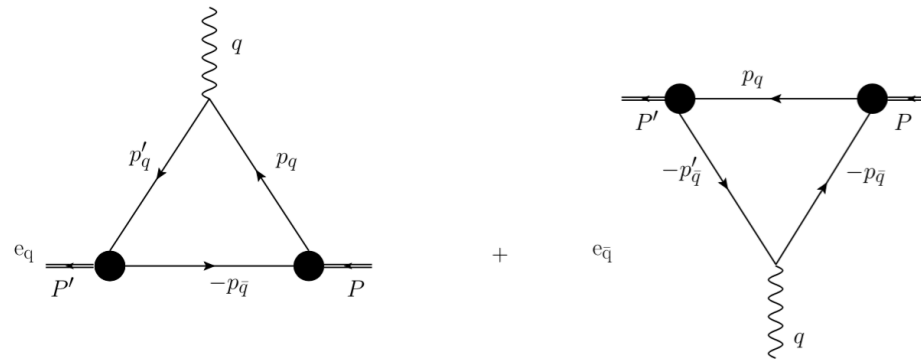
We perform a Fourier transform of the valence wf

The space-time structure of the pion in terms of loffe-time $\tilde{z} = \hat{x}^- p^+ / 2$
and the transverse coordinates $\{b_x, b_y\}$



Covariant Electromagnetic Form Factor

Among the pion observables, the electromagnetic form factor plays a relevant role for accessing the inner pion structure, since it is related to the charge density in the so-called impact parameter space.



Adopting the Impulse approximation (bare photon vertex), we have

$$(p + p')^\mu F(Q^2) = -i \frac{N_c}{4M^2 + Q^2} \int \frac{d^4k}{(2\pi)^4} \text{Tr}[(-\not{k} - m)\bar{\Phi}_2(k_2; p')(\not{p} + \not{p}')\Phi_1(k_1; p)]$$

After using the NIR and computing the traces, one obtains

$$F(Q^2) = \frac{N_c}{32\pi^2} \sum_{ij} \int_0^\infty d\gamma \int_{-1}^1 dz g_j(\gamma, z) \int_0^\infty d\gamma' \int_{-1}^1 dz' g_i(\gamma', z') \int_0^1 dy y^2 (1-y)^2 \frac{c_{ij}}{M_{cov}^8}$$

Valence Electromagnetic Form Factors

The Valence contribution to the FF is obtained from the matrix elements of the component γ^+

$$F_{val}(Q^2) = \frac{N_c}{16\pi^3} \int d^2k_{\perp} \int_{-1}^1 dz \left[\psi_{\uparrow\downarrow}^*(\gamma', z) \psi_{\uparrow\downarrow}(\gamma, z) + \frac{\vec{k}_{\perp} \cdot \vec{k}'_{\perp}}{\gamma\gamma'} \psi_{\uparrow\uparrow}^*(\gamma', z) \psi_{\uparrow\uparrow}(\gamma, z) \right]$$

$$F_{val}(0) = p_{val}.$$

where $\vec{k}'_{\perp} = \vec{k}_{\perp} + \frac{1}{2}(1+z)\vec{q}_{\perp}$

Total FF (Drell-Yan Frame): $F(Q^2) = \sum_{n=2}^{\infty} F_n(Q^2) = F_{val}(Q^2) + F_{nval}(Q^2)$

where $F_n(Q^2)$ represents the contribution of the n-th Fock component

Asymptotic behavior:

$$F_{val}(Q^2)|_{Q^2 \rightarrow \infty} \sim F_{val}^{(a)}(Q^2) = \frac{N_c}{16\pi^2} \int_{-1}^1 dz \psi_{\uparrow\downarrow} \left(\frac{(1+z)^2}{4} Q^2, z \right) \int_0^{\infty} d\gamma \psi_{\uparrow\downarrow}(\gamma, z)$$

Results: pion charge radius

Ydrefors, WP, Nogueira, Frederico and Salmè **PLB** 820, 136494 (2021).

Pion charge radius and its decomposition in valence and non valence contributions.

Set	m	B/m	μ/m	Λ/m	P_{val}	f_π	r_π (fm)	r_{val} (fm)	r_{nval} (fm)
I	255	1.45	2.5	1.2	0.70	130	0.663	0.710	0.538
II	215	1.35	2	1	0.67	98	0.835	0.895	0.703

where

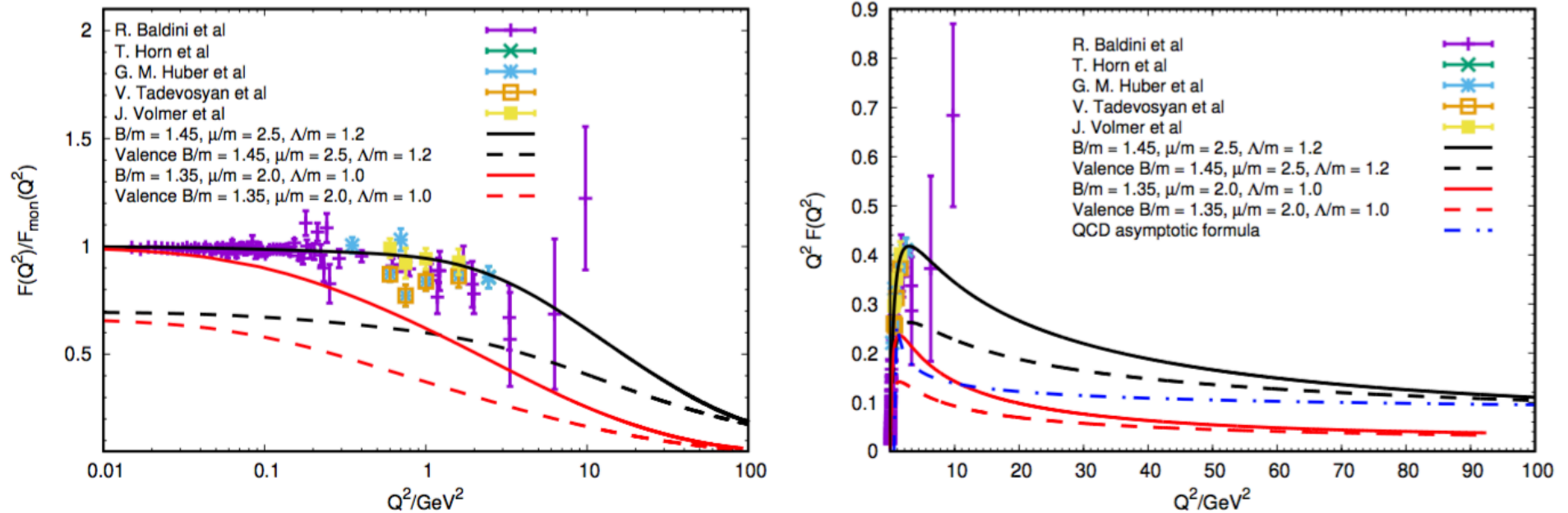
$$r_\pi^2 = -6dF(Q^2)/dQ^2|_{Q^2=0}$$

$$P_{val(nval)} r_{val(nval)}^2 = -6 dF_{val(nval)}(Q^2)/dQ^2|_{Q^2=0}$$

The set I is in fair agreement with the PDG value: $r_\pi^{PDG} = 0.659 \pm 0.004$ fm

Form factor vs Q^2

Ydrefors, WP, Nogueira, Frederico and Salmè **PLB** 820, 136494 (2021).



$$m_q = 255 \text{ MeV}, m_g = 637.5 \text{ MeV and } \Lambda = 306 \text{ MeV}$$

Good agreement with experimental data (black curve).

For high Q^2 we obtain the valence dominance (dashed black curve)

Our results recover the pQCD for large Q^2 – Blue curve vs Black curve

Phenomenological Model (Recent Developments)

In collaboration with Duarte, Frederico, Ydrefors

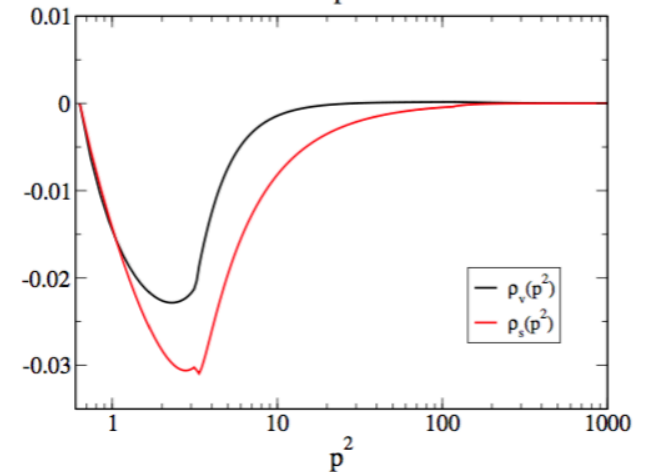
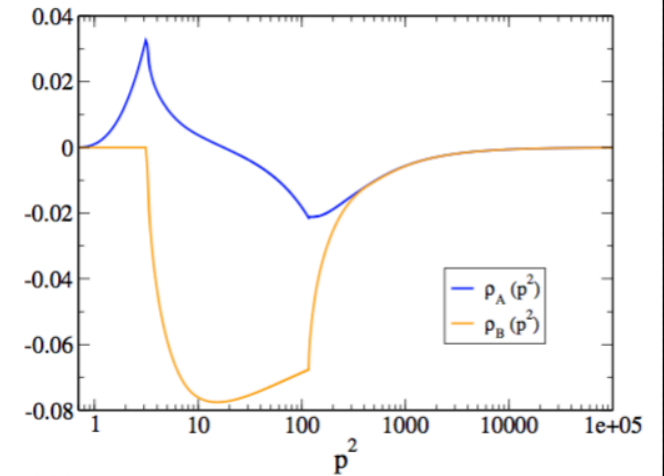
Spectral densities evaluated by solving the DSE the method described previously as inputs for the pion Bethe-Salpeter equation.

$$\Psi_{\pi}(k; p) = S_F(k_q) \Gamma_{\pi}(k; p) S_F(k_{\bar{q}})$$

$$\begin{aligned} S_F(k) &= \frac{i}{A(k^2)\not{k} - B(k^2)} \\ &= i [S_v(k^2)\not{k} + S_s(k^2)] \end{aligned}$$

$$S_v(k^2) = \frac{R}{k^2 - \bar{m}_0^2 + i\epsilon} + \int_0^{\infty} ds \frac{\rho_v(s)}{k^2 - s + i\epsilon}$$

$$S_s(k^2) = \frac{R\bar{m}_0}{k^2 - \bar{m}_0^2 + i\epsilon} + \int_0^{\infty} ds \frac{\rho_s(s)}{k^2 - s + i\epsilon}$$



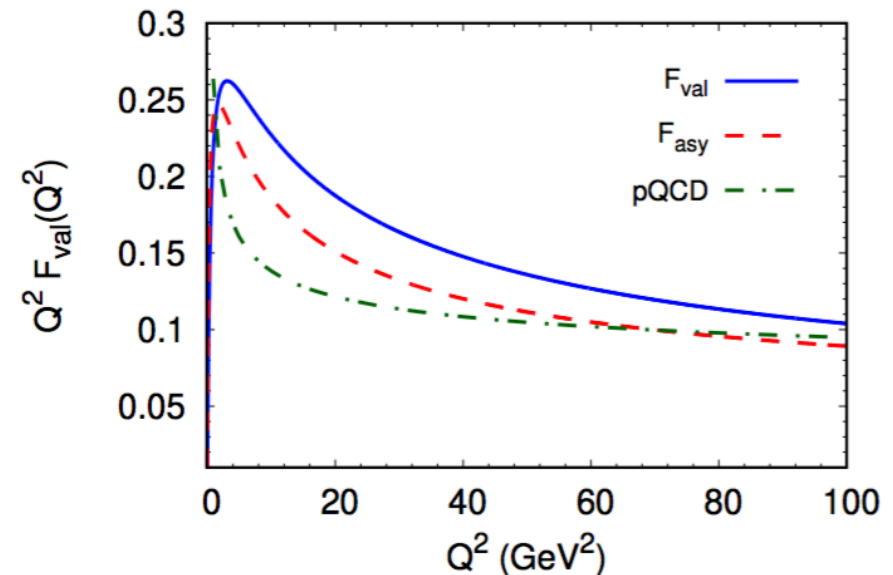
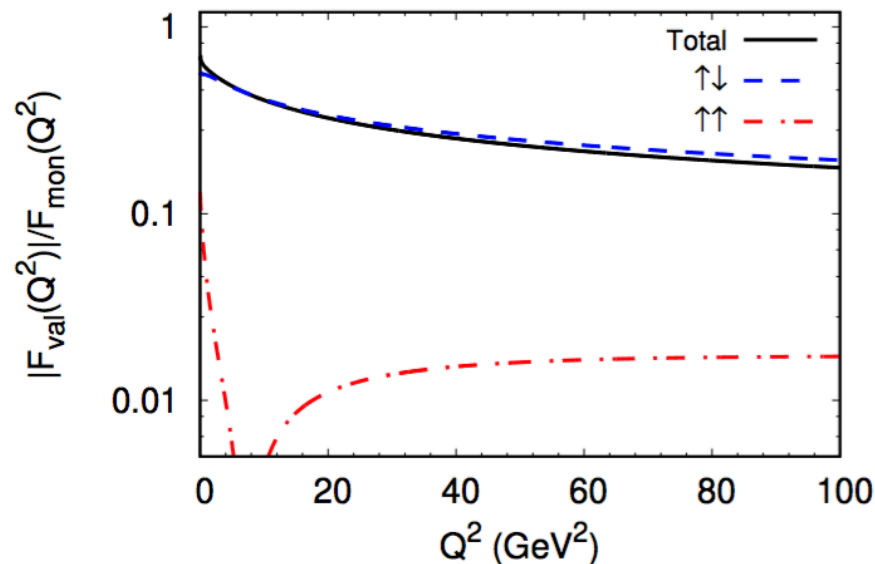
Conclusions and Perspectives

- We present a method for solving the fermionic BSE in Minkowski space and how to treat the expected singularities.
- We obtain the Valence Probability, the Momentum Distributions, Decay constant, charge radius and Electromagnetic Form Factor.
- Furthermore, the image of the pion in the configuration space has been constructed. This 3D imaging is in line with the goal of the future Electron Ion Collider.
- The beyond-valence contributions are important. The valence probability is of the order of 70%.
- We intend to calculate other Hadronic observables: TMD, GPD.
- Future plan is to include dressing functions for quark and gluon propagators and a more realistic quark-gluon vertex.

Spin configurations contributions

Ydrefors, WP, Nogueira, Frederico and Salmè **PLB** 820, 136494 (2021).

Within the BSE approach we can calculate the contribution to the valence FF from the 2 different spin configurations present in the pion.



For zero momentum transfer, the pure relativistic Spin-aligned configuration contributes with 20%.

Zero in spin-aligned FF is due to relativistic spin-orbit coupling that produces the term $\boldsymbol{\kappa} \cdot \boldsymbol{\kappa}'$, which flips the sign around $Q^2 \sim 8 \text{ GeV}^2$

For large Q^2 , the difference between the exact formula, the asymptotic expression and pQCD becomes small.

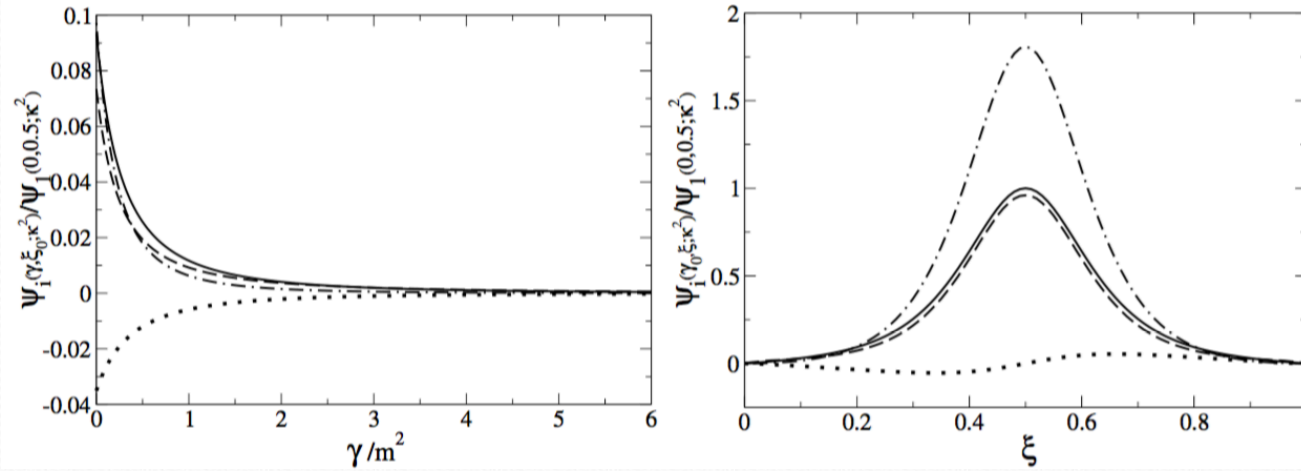


Backup

LF amplitudes

WdP, Frederico, Salme, Viviani and Pimentel – EPJC 77: 764

Weak Binding



Strong Binding

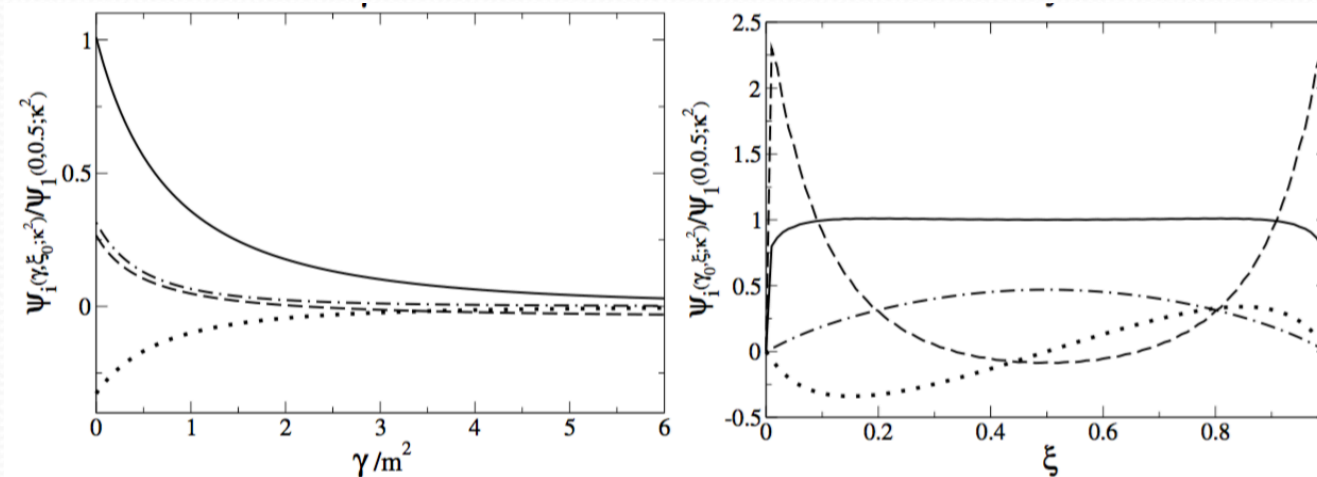
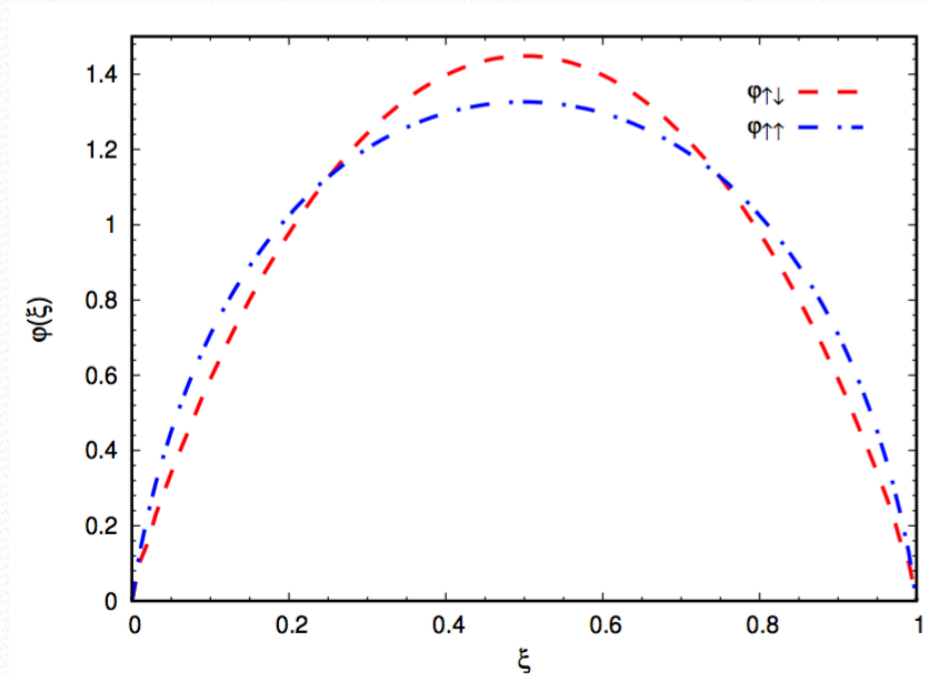


Fig. 5 LF amplitudes for weak ($B/m = 0.1$) and strong binding ($B/m = 1.0$) with mass $\mu/m = 0.15$. Solid line: ψ_1 . Dashed line: ψ_2 . Dotted line: ψ_3 . Dot-Dashed line: ψ_4 .

$$z = -2k^+/M$$

$$0 < \xi = (1 - z)/2 < 1$$

Pion Distribution Amplitude

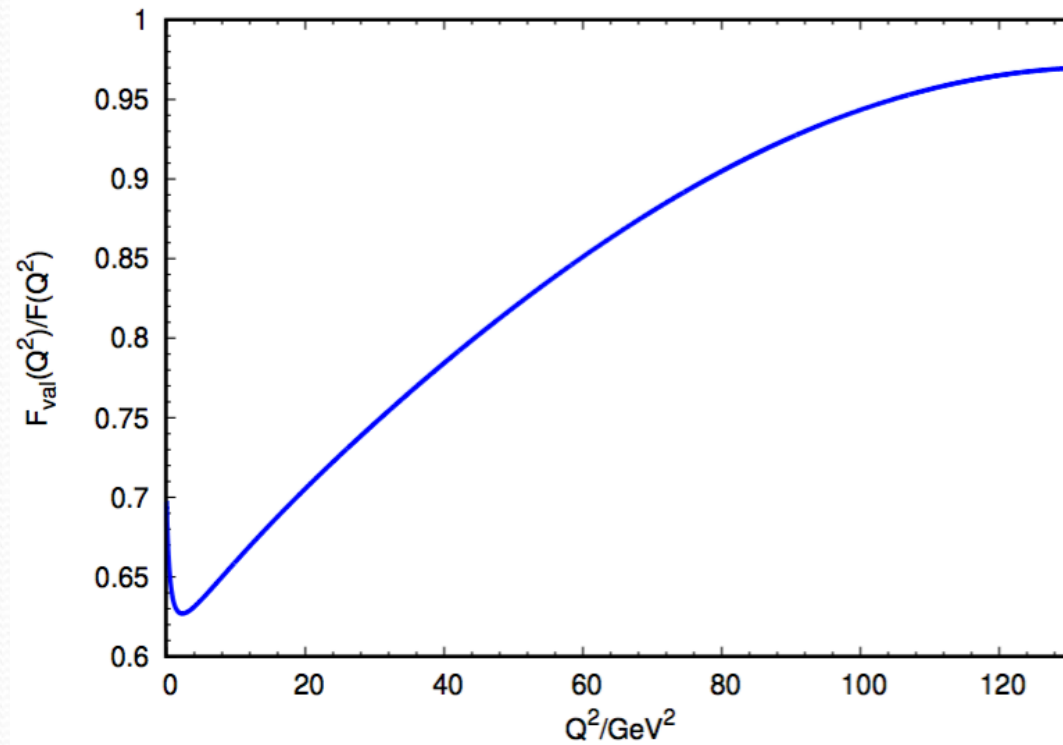


The spin components of the DA, defined by

$$\phi_{\uparrow\downarrow(\uparrow\uparrow)}(\xi) = \frac{\int_0^\infty d\gamma \psi_{\uparrow\downarrow(\uparrow\uparrow)}(\gamma, z)}{\int_0^1 d\xi \int_0^\infty d\gamma \psi_{\uparrow\downarrow(\uparrow\uparrow)}(\gamma, z)}$$

Aligned component (blue) more wide than the anti-aligned one (red).

Valence vs Covariant FF



Beyond-valence contributions are important for small Q^2

Quantitative results

To solve the BSE we have 3 input parameters:

- i) the constituent quark mass (m), ii) the gluon mass (μ)
- iii) the scale of the interaction vertex (Λ)

We consider the pion mass of 140 MeV.

The Binding energy is $B = 2m - m_\pi$

Pion Decay Constant

In terms of the BS amplitude, we can write the Pion Decay Constant as:

$$i p^\mu f_\pi = N_c \int \frac{d^4 k}{(2\pi)^4} \text{Tr}[\gamma^\mu \gamma^5 \Phi(p, k)]$$

Contracting with p_μ and using the BSA decomposition we have

$$i M^2 f_\pi = -4 M N_c \int \frac{d^4 k}{(2\pi)^4} \phi_2(k, p)$$

which can be expressed as

$$f_\pi = i \frac{\pi N_c}{(2\pi)^3} \int_0^\infty d\gamma \int_{-1}^1 dz \psi_{\uparrow\downarrow}(\gamma, z)$$

Valence Electromagnetic Form Factor

The valence electromagnetic FF, obtained from the matrix element of γ^+ , can be written as

$$F_{val}(Q^2) = \frac{N_c}{16\pi^3} \int d^2k_{\perp} \int_{-1}^1 dz \left[\psi_{\uparrow\downarrow}^*(\gamma', z) \psi_{\uparrow\downarrow}(\gamma, z) + \frac{\vec{k}_{\perp} \cdot \vec{k}'_{\perp}}{\gamma\gamma'} \psi_{\uparrow\uparrow}^*(\gamma', z) \psi_{\uparrow\uparrow}(\gamma, z) \right];$$
$$F_{val}(0) = p_{val},$$

where $\vec{k}'_{\perp} = \vec{k}_{\perp} + \frac{1}{2}(1+z)\vec{q}_{\perp}$ and e.g. $\gamma = |k_{\perp}|^2$.

Total FF is $F(Q^2) = F_{val}(Q^2) + F_{nval}(Q^2)$.

Asymptotically,

$$F_{val} \sim \frac{N_c}{16\pi^2} \int_{-1}^1 dz \psi_{\uparrow\downarrow} \left(\frac{(1+z)^2}{4} Q^2, z \right) \int_0^{\infty} d\gamma \psi_{\uparrow\downarrow}(\gamma, z); \quad Q^2 \rightarrow \infty,$$

Valence Momentum Distributions

The valence longitudinal and transverse LF-momentum distribution densities are obtained by properly integrating the Valence probability density.

The valence longitudinal-momentum distribution is:

$$\phi(\xi) = \phi_{\uparrow\downarrow}(\xi) + \phi_{\uparrow\uparrow}(\xi)$$

with

$$\phi_{\uparrow\downarrow(\uparrow\uparrow)}(\xi) = \int_0^\infty d\gamma \mathcal{P}_{\uparrow\downarrow(\uparrow\uparrow)}(\gamma, z)$$
$$\xi = k^+ / p^+$$

The valence transverse-momentum distribution is:

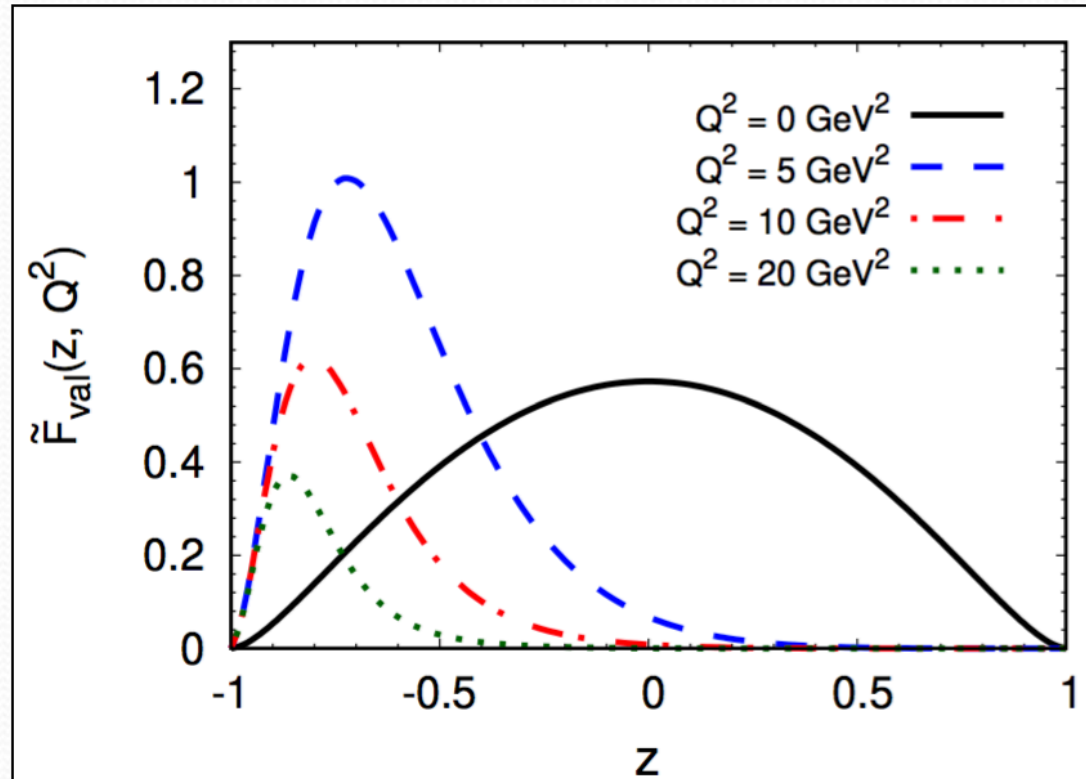
$$P(\gamma) = P_{\uparrow\downarrow}(\gamma) + P_{\uparrow\uparrow}(\gamma)$$

with

$$P_{\uparrow\downarrow(\uparrow\uparrow)}(\gamma) = \int_{-1}^1 dz \mathcal{P}_{\uparrow\downarrow(\uparrow\uparrow)}(\gamma, z)$$

$$\gamma = k_\perp^2$$

Sliced Valence FF



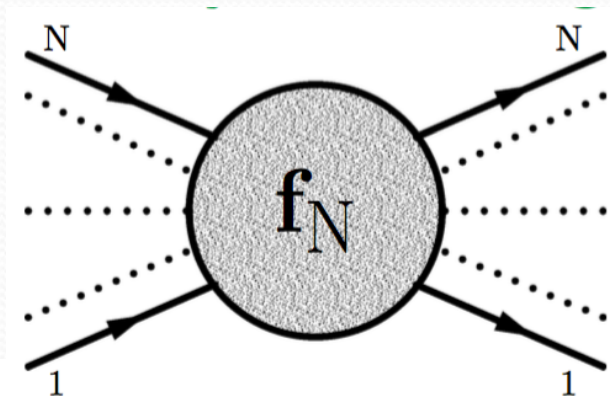
Sliced valence FF defined through

$$F_{val}(Q^2) = \int_{-1}^1 dz \tilde{F}_{val}(z, Q^2)$$

Sliced FF symmetric for $Q^2 = 0$.

Nakanishi Integral Representation

Let's take a connected Feynman diagram (G) with N external momenta p_i , n internal propagators with momenta l_j and masses m_j and k loops.



The transition amplitude is given by (scalar theory)

$$f_G(p_i) = \prod_{r=1}^k \int d^4 q_r \frac{1}{(l_1^2 - m_1^2 + i\epsilon) \cdots (l_n^2 - m_n^2 + i\epsilon)}$$

Feynman parametrization $\frac{1}{A_1 \cdots A_n} = (n-1)! \prod_{i=1}^n \int_0^1 d\alpha_i \frac{\delta(1 - \sum \alpha_i)}{\sum_{i=1}^n \alpha_i A_i}$

$$l_j = \sum_{r=1}^k b_{jr} q_r + \sum_{i=1}^N c_{ji} p_i$$

We obtain

$$f_G(p_i) = \frac{(i\pi)^k (n-2k-1)!}{(n-1)!} \prod_{i=1}^n \int_0^1 d\alpha_i \frac{\delta(\sum \alpha_i - 1)}{U^2 (\sum_{ii'} e_{ii'} p_i p_{i'} - \sum_{i=1}^n \alpha_i m_j^2 + i\epsilon)^{n-2k}}$$

The denominator is a linear combination of the scalar product of the external momenta and the masses.

The coefficients and the exponent $(n-2k)$ depends on the particular Feynman diagram.

Nakanishi Integral Representation

After some change of variables we can write

$$f_G(p_i) = \prod_h \int_0^1 dz_h \int_0^\infty d\chi \frac{\delta(1 - \sum_i z_i) \phi_G^{(n-2k)}(z, \chi)}{(\sum_i z_i s_i - \chi + i\epsilon)^{n-2k}}$$

Performing integration by parts, we have the integral representation

$$f_G(p_i) = \prod_h \int_0^1 dz_h \int_0^\infty d\chi \frac{\delta(1 - \sum_i z_i) \phi_G^{(1)}(z, \chi)}{(\sum_i z_i s_i - \chi + i\epsilon)}$$

where

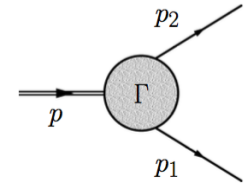
$$\phi_G^{(1)}(\chi, z_h) = (-1)^{n-2k-1} \frac{\partial^{n-2k-1}}{\partial \chi^{n-2k-1}} \phi_G^{(n-2k)}(\chi, z_h)$$

The dependence upon the details of the diagram moves from the **denominator** to the **numerator**. We obtain the **same** formal expression for the denominator of **any diagram**.

Nakanishi Integral Representation

To represent the BSA, we consider the constituent particles with momentum p_1, p_2 and the bound-state with momentum p .

$$p = p_1 + p_2 \quad k = (p_1 - p_2)/2$$



$$f_3(p_i) = \prod_h \int_0^1 dz_h \delta(\sum_h z_h - 1) \int_{0^-}^{\infty} d\chi \frac{\phi_3^{(1)}(\chi, z_h)/(z_1 + z_2)}{(k^2 + p \cdot k \frac{(z_1 - z_2)}{(z_1 + z_2)} + \frac{M^2(z_1 + z_2 + 4z_3) - \chi}{(z_1 + z_2)} + i\epsilon)}$$

Using the identities

$$1 = \int d\gamma' \delta(\gamma' + \left(\frac{M^2(z_1 + z_2 + 4z_3) - \chi}{(z_1 + z_2)} \right))$$

$$1 = \int_{-1}^1 dz' \delta(z' - \left(\frac{z_1 - z_2}{z_1 + z_2} \right))$$

we obtain the NIR

$$f_3(p, k) = \int d\gamma' \int_{-1}^1 dz' \frac{g^{(1)}(\gamma', z')}{k^2 + z'p \cdot k - \gamma' + i\epsilon}$$

where

$$g^{(1)}(\gamma', z') = \prod_h \int_0^1 dz_h \delta(\sum_h z_h - 1) \int_{0^-}^{\infty} d\chi \times \frac{\phi_3^{(1)}(\chi, z_h)}{(z_1 + z_2)} \delta(z' - \left(\frac{z_1 - z_2}{z_1 + z_2} \right)) \delta(\gamma' + \left(\frac{M^2(z_1 + z_2 + 4z_3) - \chi}{(z_1 + z_2)} \right))$$